

Thermal Diffusion And Inclined Magnetic Field Effects On Mhd Free Convection Flow Of Casson Fluid Past An Inclined Plate In Conducting Field

C Pavan Kumar¹, K Raghunath^{2*}, M Obulesu³

¹Assistant Professor, Department of Humanities and Sciences(Mathematics), PACE Institute of Technology & Science, Ongole, A.P, Pin-523272, India. email: dr_pavankumar@pace.ac.in

²Assistant Professor, Department of Humanities and Sciences(Mathematics), Bheema Institute of Technology & Science, Adoni, A.P, Pin-518301, India. email:kraghunath25@gmail.com

³Research Associate, Department of Mathematics, S.K.University, Anantapur, A.P, Pin 515003, India, email: mopuriobulesu1982@gmail.com

Article History: Received: 10 January 2021; Revised: 12 February 2021; Accepted: 27 March 2021; Published online: 4 June 2021

Abstract

Analytical solution of thermal diffusion and diffusion thermo effects on MHD Casson fluid flow past an oscillating inclined plate embedded through porous medium in the presence of thermal radiation, aligned magnetic field and chemical reaction is obtained. The governing non-dimensional equations are solved using perturbation technique and the solutions are presented in closed form. In order to get a perfect understanding of the physics of the problem we obtained numerical results using Matlab software and clarified with the help of graphical illustrations. With the help of velocity, temperature and concentration, Skin friction, Nusselt number and Sherwood number are obtained and represent through tabular form. Casson parameter is inversely proportional to the yield stress and it is observed that for the large value of Casson parameter, the fluid is close to the Newtonian fluid where the velocity is less than the non-Newtonian fluid. The intensification in values of Soret number produces a raise in the mass buoyancy force which results an increase in the value of velocity. Comparison of the results presented. We have an excellent agreement with the existed results.

Keywords: Casson fluid, Soret effect, MHD, Radiation, Heat absorption, Chemical reaction, Porous medium.

1. Introduction:

The Newtonian theory has worked extremely well in explaining numerous physical phenomena in diverse fields of fluid dynamics; this entices us to comment that the most of the fluids at least in ordinary situations perform similar to Newtonian fluids. But in the modern years, in particular with the materialization of polymers, it has been established that there are fluids which illustrate a different deviation from Newtonian theory. Such fluids are known as non-Newtonian fluids. The non-Newtonian fluids are generally classified into the following categories, which are Maxwell fluids, dilatants fluids, Reiner-Rivlin fluids, purely viscous fluids, viscoelastic fluids as well as perfectly plastic materials, couple stress fluid, power law fluids, viscoelastic fluids, pseudo-plastic fluids, Casson fluid, micropolar fluid, etc.. Currently, in this paper, it has been studied on Casson fluid flow past an oscillating vertical plate embedded through porous medium in the presence of thermal radiation aligned magnetic field and chemical reaction. Non-Newtonian fluid exits non-linear relationships between the shear stress and rate of shear strain. It has an extensive variety of applications in engineering and industry, especially in the extraction of crude oil from petroleum products. Casson fluid is classified as the most popular non-Newtonian fluid which has several applications in food processing, metallurgy, drilling operations and bio-engineering operations. Shaw et al. [1] presented the concept of Pulsatile Casson fluid flow through a stenosed bifurcated artery. Nadeem et al. [2] presented the concept of MHD three dimensional Casson fluids past a porous linearly stretching sheet. Hayat et al. [3] elaborated the three-dimensional stretched flow of Jeffrey fluid with variable thermal radiation. Thiagarajan and Senthilkumar [4] studied the DTM-Pade approximants of MHD boundary-Layer flow of a Casson fluid over a Shrinking Sheet. Mukhopadhyaya [5] elaborated the effects of slip on unsteady mixed convective flow and heat transfer past a stretching surface. MHD three-dimensional flow and heat transfer over a stretching surface in a viscoelastic fluid are invented by Ahmad and Nazar [6]. Bhattacharya et al. [7] investigated the analytical solutions

for the boundary layer stagnation point flow and heat transfer towards the shrinking sheet. Kameswaran et al. [8] discussed the dual solutions of Casson fluid flowing over a stretching or shrinking sheet.

The existing approach in the applications of magnetohydrodynamic (MHD) is in the direction of the strong magnetic fields to obtain the impact of electromagnetic force into consideration. Therefore, the influence of Hall and ion-slip current is critical because they contain excellent effect on the current density. The influence of Hall and ion-slip current has plentiful applications, particularly if included with heat transfer, such as in magnetic resonance imaging (MRI), cancer therapy, magnetic drug targeting, Hall accelerators, heating elements, refrigeration coils, and power generators and so on. This helps to generate the images of arteries to investigate the continuation of stenosis or any other circumstances in the arteries of the brain, pumping of blood. Moreover, the examination of the effect of the magnetic field in conjunction by means of the influence of Hall as well as ion slip on the blood flow in vein has been established to be very helpful and valid in magnetic resonance angiography (MRA). Most recently, keeping the above applications, Ahammad et al. [8] have investigated Hall and ion slip impacts on unsteady MHD convective rotating flow of Heat generating/absorbing second-grade fluid. Veera Krishna M et al. [9] have possessed Heat and mass transfer on MHD Chemically Reacting flow of a Micro-polar fluid through a Porous Medium with Hall effects. Special Topics & Reviews in Porous Media. Krishna M Veera et al. [10] have researched Heat, and mass transfer on Unsteady MHD Oscillatory flow of Second-grade fluid through the porous medium between two vertical plates fluctuating Heat Source/Sink and Chemical react. Veera Krishna et al. [11] have discussed Heat and Mass transfer on Free Convective Flow of a Micro-polar fluid through a Porous surface with Inclined Magnetic Field and Hall effects. Krishna Veera et al. [12] have analyzed Heat and mass transfer on the MHD flow of Second-grade fluid through a porous medium over a semi-infinite vertical stretching sheet. A very recently Obulesu et al. [13] have analyzed Radiation Absorption Effects on MHD Jeffrey fluid flow Past a Vertical Plate through a Porous Medium in Conducting Field. Raghunath et al. [14] have possessed Heat and mass transfer on an unsteady MHD flow through porous medium between two porous vertical plates. Very recently Obulesu et al. [15] have studied Hall current effects on MHD convective flow past a porous plate with thermal radiation, chemical reaction with radiation absorption. Raghunath et al. [16] have discussed Heat and mass transfer on MHD flow of Non-Newtonian fluid over an infinite vertical porous plate. Raghunath et al. [17] have possessed Heat and mass transfer on Unsteady MHD flow of a second grade fluid through porous medium between two vertical plates. Raghunath et al. [18] have studied Hall Effects on MHD Convective Rotating Flow of through a Porous Medium past Infinite Vertical Plate. Raghunath et al. [19] have discussed Heat and Mass Transfer on Unsteady MHD Flow of a Visco-Elastic Fluid Past an Infinite Vertical Oscillating Porous Plate. GVN Prasad et al. [20] have expressed MHD flow of a Visco-elastic fluid over an unbounded rotating porous plate with Heat source and Chemical reaction. Suresh babu et al. [21] has studied Finite Element Analysis of Free Convection Heat Transfer Flow in a Vertical Conical Annular Porous Medium.

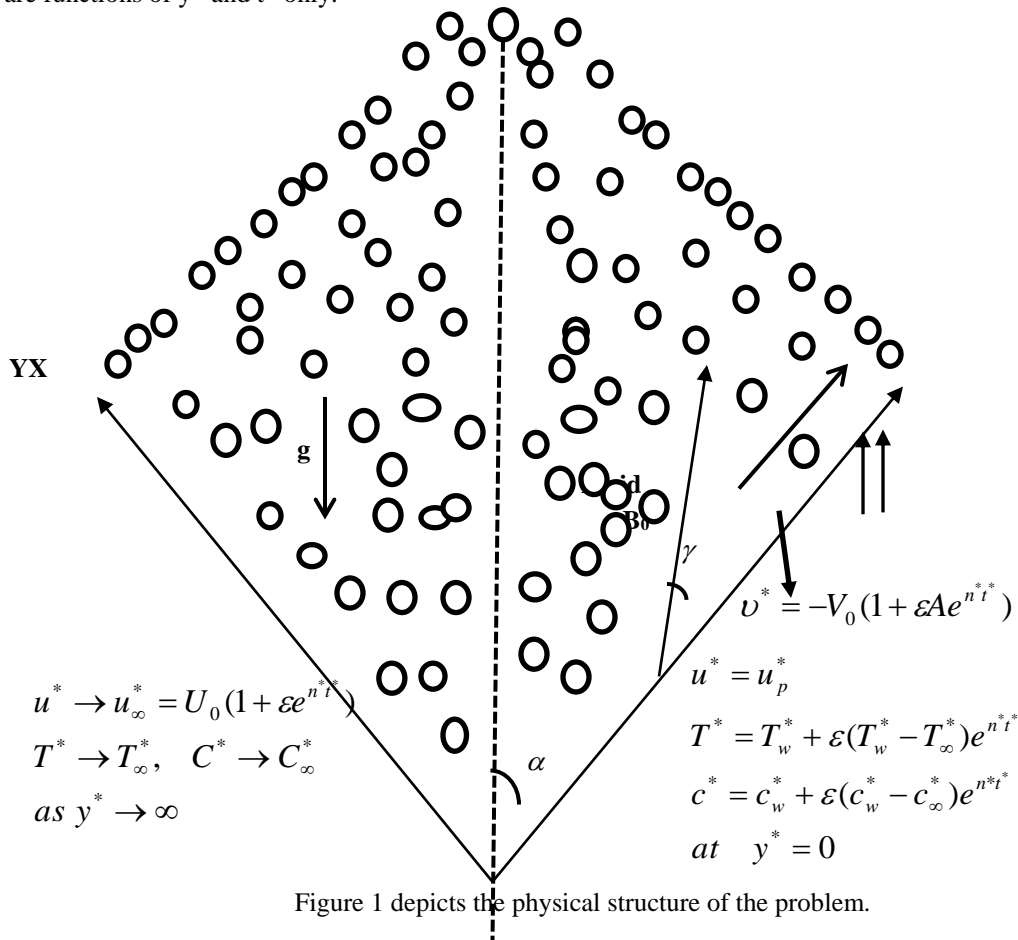
Thermal radiation has multitudinous remarkable applications because of the approach in which radiant emission relies on temperature. Subsequently, radiation contributes significantly to energy transfer in furnaces, combustion chambers, fires and to energy emission, such as that of a nuclear explosion. Radiative behavior governs the temperature distribution within the sun and the solar emission. The nature devices are designed to operate at high temperature levels to achieve good thermal efficiency. Hence, radiation must be contemplated in calculating thermal effects in rocket nozzles, power plants, engines and high-temperature heat exchangers, geophysics, various propulsion devices for missiles, photo ionization, gas turbines, combustion of fossil fuels, nuclear power plants, liquid metal fluids, plasma wind tunnels and aircraft, space vehicles, satellites, and so on. The effects of thermal radiation on MHD free convective fluid over an impulsively started infinite vertical plate embedded in a porous medium under dissimilar flow conditions were investigated by various explorers. Prabhakar Reddy et al. [22] reported the influence of thermal radiation on MHD double-diffusion flow past a surface surrounded in a porous medium by means of chemical reaction. In this paper, it was concluded that thermal radiation certainly affects the temperature and consequently the velocity and hence the skin friction. Okelo J et al. [23] considered the influence of radiation absorption and heat generation effects on viscous incompressible fluid flow past an infinite permeable plate. Influence of radiation on unsteady MHD mixed convective fluid flow past an infinite perpendicular plate by means of Soret and Dufour effects was discussed by Vedavathi et al. [24]. Gnaneswara Reddy et al. [25]

investigated the influence of thermal radiation and heat source on MHD mixed convective slip flow in a porous medium in the presence of chemical reaction as well as Ohmic heating. Choudhury and Ahmed [26] studied Soret Effect on Transient MHD Convective Flow past a Semi-infinite Vertical Porous Plate with Heat Sink and Chemical Reaction. Recently, Rajakumar et al. ([27] and [28]) studied analytically an impact of thermal radiation as well as chemical reaction on MHD free convective dissipative fluid flow past a semi-infinite moving non-parallel permeable palate. In the above examination, viscoelastic fluid was not contemplated. Obulesu et al. [31-33] have studied in the MHD double diffusive visco-elastic fluid flow past an infinite vertical porous plate under the influence of radiation absorption.

Therefore our work can be considered as extension of Ref. [26]. By consideration of Cassion fluid, Radiation, Aligned magnetic field and Inclined porous vertical plates. So Novelty of this paper is discussion of analytical solutions using Perturbation method and numerical solution using Matlab software of the unsteady natural convective Casson fluid flow past over an oscillating vertical plate in the presence of a radiation, Aligned magnetic field, chemical reaction, thermal diffusion and heat generation with ramped wall temperature and ramped surface concentration through porous medium.

2. Mathematical Formulation

Let us consider a flow of an incompressible viscous electrically conducting fluid past an infinite vertical porous plate. We introduce a Cartesian coordinate system (x^*, y^*, z^*) with X axis along the infinite vertical plate, Y axis normal to the plate and Z axis along the width of the plate. Initially the plate and the fluid were at same temperature T_∞^* with concentration level C_∞^* at all points. At time $t^* > 0$ the plate temperature is suddenly raised to $T_w^* + \varepsilon(T_w^* - T_\infty^*)e^{n^*t^*}$ and the concentration level at the plate rose to $C_w^* + \varepsilon(C_w^* - C_\infty^*)e^{n^*t^*}$. A uniform magnetic field is applied normal to the plate. Due to semi-infinite plane surface assumptions, all the flow variables except pressure are functions of y^* and t^* only.



Our investigation is restricted to the following assumptions:

- i) All the fluid properties are considered constants except the influence of the variation in density in the buoyancy force term.
- ii) Viscous dissipation and Ohmic dissipation of energy are negligible.
- iii) It is assumed that there is no applied voltage which implies the absence of an electrical field. The transversely applied magnetic field and magnetic Reynolds number are assumed to be very small so that the induced magnetic field and the Hall Effect are negligible.
- iv) Induced electric field is neglected. By considering the above assumptions, the governing equations are given by
- v) The rheological equation of state for an isotropic incompressible flow of a casson fluid [20] can be expressed as:

$$\tau_{ij} = \begin{cases} \left(\mu_B + \frac{P_y}{\sqrt{2\pi}} \right) e_{ij}, \pi > \pi_c, \\ \left(\mu_B + \frac{P_y}{\sqrt{2\pi_c}} \right) e_{ij}, \pi < \pi_c, \end{cases} \quad (7)$$

- vi) In equation (7), $\pi = e_{ij}e_{ij}$, Where e_{ij} are the (i, j) th Component of the deformation rate, π is the product of the deformation rate with itself, π_c is a critical value of this product based on the non-Newtonian model, μ_B is the plastic dynamic viscosity of the non-Newtonian fluid and P_y the yield stress of the fluid.

All the basic governing equations [8-11] and boundary conditions [12] can be followed by Chawdary et al. [26].

$$\frac{\partial v^*}{\partial y^*} = 0 \rightarrow v^* = -v_0 (v_0 > 0) \quad (8)$$

$$\frac{\partial u^*}{\partial t^*} + v^* \frac{\partial u^*}{\partial y^*} = -\frac{1}{\rho} \frac{\partial p^*}{\partial x^*} + \mathcal{G} \left(1 + \frac{1}{\lambda} \right) \frac{\partial^2 u^*}{\partial y^{*2}} + g\beta(T^* - T_\infty^{**}) \text{Cos } \alpha + gB^*(C^* - C_\infty) \text{Cos } \alpha - \frac{\sigma B_0^2}{\rho} \text{Sin}^2 \gamma u^* - \frac{\mathcal{G}u^*}{k^*} \quad (9)$$

$$\frac{\partial T^*}{\partial t^*} + V^* \frac{\partial T^*}{\partial y^*} = \frac{K}{\rho C_p} \frac{\partial^2 T^*}{\partial y^{*2}} - \frac{1}{\rho C_p} \frac{\partial q_r^*}{\partial y^*} - \frac{Q^*}{\rho C_p} (T^* - T_\infty^*) \quad (10)$$

$$\frac{\partial C^*}{\partial t^*} + V^* \frac{\partial C^*}{\partial y^*} = D_M \frac{\partial^2 C^*}{\partial y^{*2}} - K^*(C^* - C_\infty^*) + \frac{D_M K_T}{T_M} \frac{\partial^2 T^*}{\partial y^{*2}} \quad (11)$$

Under the above assumptions, the appropriate boundary conditions for the distributions of velocity, temperature and concentration are given by

$$\begin{aligned}
 u^* &= u_p^*, \quad T^* = T_w^* + \varepsilon(T_w^* - T_\infty^*)e^{n^*t^*}, \quad C^* = C_w^* + \varepsilon(C_w^* - C_\infty^*)e^{n^*t^*} \quad \text{at } y^* = 0 \\
 u^* &\rightarrow u_\infty^* = U_0(1 + \varepsilon e^{n^*t^*}), \quad T^* \rightarrow T_\infty^* \quad C^* \rightarrow C_\infty^* \quad \text{as } y^* \rightarrow \infty
 \end{aligned}
 \tag{12}$$

The equation of continuity yields that V^* is either a constant or some function of time, hence we assume that

$$V^* = -V_0(1 + A\varepsilon e^{n^*t^*})
 \tag{13}$$

Where A is a real positive constant, ε and $A\varepsilon$ are small less than unity, V_0 is the scale of the suction velocity which has a non-zero positive constant.

Outside the boundary layer, Equation (9) gives

$$-\frac{1}{\rho} \frac{\partial p^*}{\partial x^*} = \frac{\partial u_\infty^*}{\partial t^*} + \frac{\nu}{k^*} U_\infty^* + \frac{\sigma B_0^2}{\rho} U_\infty^* \sin^2 \gamma
 \tag{14}$$

We consider a mathematical model, for an optically thin limit gray gas near equilibrium in the form given by Cramer and Pai [29]. Later Grief et al. [30]

$$\frac{\partial q_r^*}{\partial y^*} = 4(T^* - T_w^*)I
 \tag{15}$$

Where $I = \int_0^\infty K_{\lambda\omega} \left(\frac{\partial eb\lambda}{\partial T} \right) d\lambda$, $K_{\lambda\omega}$ the absorption coefficient at the wall and $eb\lambda$ is Planck's function.

To normalize the mathematical model of the physical problem, we introduce the following non-dimensional quantities and parameters

$$\begin{aligned}
 u &= \frac{u^*}{U_0}, \quad y = \frac{U_0 y^*}{\mathcal{G}}, \quad T = \frac{T^* - T_\infty^*}{T_w^* - T_\infty^*}, \quad C = \frac{C^* - C_\infty^*}{C_w^* - C_\infty^*}, \quad \text{Pr} = \frac{\mu C_p}{K_T}, \quad \text{Sc} = \frac{\mathcal{G}}{D}, \quad M = \frac{\sigma B_0^2 \mathcal{G}}{\rho U_0^2}, \\
 Gr &= \frac{\mathcal{G} g \beta_T (T_w^* - T_\infty^*)}{U_0^3}, \quad Gm = \frac{\mathcal{G} g \beta_c (C_w^* - C_\infty^*)}{U_0^3}, \quad K = \frac{U_0^2 K_0^*}{\mathcal{G}^2}, \quad t = \frac{t^* U_0^2}{4\mathcal{G}}, \quad h = \frac{U_0^2 L_1}{\mathcal{G}}, \\
 K &= \frac{\mathcal{G} K_c^*}{U_0^2}, \quad R = \frac{4I^* \mathcal{G}}{\rho C_p v_0^2}, \quad Q = \frac{Q_1 v}{U_0^2}, \quad S_0 = \frac{D_1 (T_w^* - T_\infty^*)}{\mathcal{G} (C_w^* - C_\infty^*)}, \quad R = \frac{4\mathcal{G} n^*}{U_0^2}, \quad F = \frac{4I_1 v}{\rho C_p v_0^2}
 \end{aligned}
 \tag{16}$$

The non-dimensional form of the equations (9) to (11) are

$$\frac{\partial u}{\partial t} - (1 + A\varepsilon e^{n^*t^*}) \frac{\partial u}{\partial y} = \frac{dU_\infty}{dt} + \lambda_1 \frac{\partial^2 u}{\partial y^2} + Gr \theta \cos \alpha + Gm \phi \cos \alpha + \xi (U_\infty - u)
 \tag{17}$$

Where $N = (M \sin^2 \gamma + 1/k)$, $\lambda_1 = \left(1 + \frac{1}{\lambda}\right)$

$$\frac{\partial \theta}{\partial t} - (1 + A \varepsilon e^{-nt}) \frac{\partial \theta}{\partial y} = -\frac{1}{Pr} \frac{\partial^2 \theta}{\partial y^2} - \chi \theta \tag{18}$$

Where $\chi = F + Q$

$$\frac{\partial \phi}{\partial t} - (1 + A \varepsilon e^{-nt}) \frac{\partial \phi}{\partial y} = \frac{1}{Sc} \frac{\partial^2 \phi}{\partial y^2} + Sr \frac{\partial^2 \phi}{\partial y^2} - K \phi \tag{19}$$

The corresponding boundary conditions are given by

$$\begin{aligned} u = U_p \quad \theta = 1 + \varepsilon e^{-nt} \quad \phi = 1 + \varepsilon e^{-nt}, \quad \text{at } y = 0 \\ U \rightarrow U_\infty = 1 + \varepsilon e^{-nt}, \quad \theta \rightarrow 0, \quad \phi \rightarrow 0 \quad \text{as } y \rightarrow \infty \end{aligned} \tag{20}$$

3. Method of Solution

In order to solve the non-linear partial differential equations (17)-(19) subject to the condition (20), the expressions for the velocity, temperature and concentration are assumed to be of the asymptotic form

$$\begin{aligned} U(y,t) &= u_0(y) + \varepsilon u_1(y)e^{-nt} + O(\varepsilon^2) \\ T(y,t) &= \theta_0(y) + \varepsilon \theta_1(y)e^{-nt} + O(\varepsilon^2) \\ C(y,t) &= \phi_0(y) + \varepsilon \phi_1(y)e^{-nt} + O(\varepsilon^2) \end{aligned} \tag{21}$$

Substituting equations (21) into equation (17)–(19) and equating the coefficients at the terms with the same powers of ε , and neglecting the terms of higher order, the following equations are obtained.

Zero order terms:

$$u_0'' \lambda_1 + u_0' - N u_0 = -Gr \cos \alpha \theta_0 - Gm \cos \alpha \phi_0 - N \tag{22}$$

$$\theta_0'' + Pr \theta_0' - \chi Pr \theta_0 = 0 \tag{23}$$

$$\phi_0'' + Sc \phi_0' - Sc K \phi_0 = Sc Sr \theta_0'' \tag{24}$$

First order terms:

$$u_1'' \lambda_1 + u_1' - (N + n) u_1 = -Gr \cos \alpha \theta_1 - Gm \cos \alpha \phi_1 - A u_0' - (N + n) \tag{25}$$

$$\theta_1'' + Pr \theta_1' - (n + \chi) Pr \theta_1 = -Pr A \theta_0' \tag{26}$$

$$\varphi_1'' + Sc \varphi_1' - Sc(K + n)\varphi_1 = -A Sc \varphi_0' - Sc Sr \theta_1'' \tag{27}$$

The corresponding boundary conditions are

$$\begin{aligned} u_0 = U_p, u_1 = 0, \theta_0 = 1, \theta_1 = 1, C_0 = 1, C_1 = 1 \quad \text{at } y = 0 \\ u_0 = 1, u_1 = 1, \theta_0 \rightarrow 0, \theta_1 \rightarrow 0, C_0 \rightarrow 0, C_1 \rightarrow 0 \quad \text{as } y \rightarrow \infty \end{aligned} \tag{28}$$

Solving equations (22) – (27) under the boundary conditions (28), the following solutions are obtained

$$u_0 = 1 + A_9 \exp(-m_5 y) + A_{10} \exp(-m_3 y) + A_{11} \exp(-m_5 y) \tag{29}$$

$$\begin{aligned} u_1 = 1 + A_{12} \exp(-m_1 y) + A_{13} \exp(-m_2 y) + A_{14} \exp(-m_3 y) + A_{15} \exp(-m_4 y) \\ + A_{16} \exp(-m_5 y) + A_{17} \exp(-m_6 y) \end{aligned} \tag{30}$$

$$\theta_0 = \exp(-m_1 y) \tag{31}$$

$$\theta_1 = A_1 \exp(-m_1 y) + A_2 \exp(-m_2 y) \tag{32}$$

$$\varphi_0 = A_3 \exp(-m_1 y) + A_4 \exp(-m_3 y) \tag{33}$$

$$\varphi_1 = A_5 \exp(-m_1 y) + A_6 \exp(-m_2 y) + A_7 \exp(-m_3 y) + A_8 \exp(-m_4 y) \tag{34}$$

Substituting equations (29)–(34) in equation (21) we obtain the velocity temperature and concentration field

$$\begin{aligned} u = (1 + A_9 \exp(-m_1 y) + A_{10} \exp(-m_3 y) + A_{11} \exp(-m_5 y)) + \varepsilon e^{nt} (1 + A_{12} \exp(-m_1 y) + \\ A_{13} \exp(-m_2 y) + A_{14} \exp(-m_3 y) + A_{15} \exp(-m_4 y) + A_{16} \exp(-m_5 y) + A_{17} \exp(-m_6 y)) \end{aligned} \tag{35}$$

$$\theta = \exp(-m_1 y) + \varepsilon e^{nt} (A_1 \exp(-m_1 y) + A_2 \exp(-m_2 y)) \tag{36}$$

$$\begin{aligned} \phi = A_3 \exp(-m_1 y) + A_4 \exp(-m_3 y) + \varepsilon e^{nt} (A_5 \exp(-m_2 y) + \\ A_6 \exp(-m_2 y) + A_7 \exp(-m_3 y) + A_8 \exp(-m_4 y)) \end{aligned} \tag{37}$$

Skin Friction:

The non-dimensional skin friction at the surface is given by

$$\begin{aligned} \tau = \left(\frac{\partial u}{\partial y} \right)_{y=0} \\ \tau = -(m_1 A_9 + m_3 A_{10} + m_5 A_{11}) \\ - \varepsilon e^{nt} (m_1 A_{12} + m_2 A_{13} + m_3 A_{14} + m_4 A_{15} + m_5 A_{16} + m_6 A_{17}) \end{aligned} \tag{38}$$

Nusselt Number:

The rate of heat transfer in terms of the Nusselt number is given by

$$Nu = -\left(\frac{\partial \theta}{\partial y}\right)_{y=0}$$

$$Nu = -m_1 - \varepsilon e^{nt} (m_1 A_1 + m_2 A_2) \tag{39}$$

Sherwood Number:

The rate of mass transfer on the wall in terms of Sherwood number is given by

$$Sh = -\left(\frac{\partial C}{\partial y}\right)_{y=0}$$

$$Sh = -(m_1 A_3 + m_3 A_4) - \varepsilon e^{nt} (m_1 A_5 + m_2 A_6 + m_4 A_7 + m_5 A_8) \tag{40}$$

4. Results and Discussion

In order to get the physical insight of the problem, we have carried out numerical calculations for non-dimensional velocity field, temperature field, concentration field, coefficient of skin friction at the plate, the rate of heat transfer and the rate of mass transfer at the plate for different values of the physical parameters involved and these are demonstrated in graphs. We assign values to the parameters as, $Sc=0.22$, $Pr=0.71$, $Gr=5$, $K=0.5$, $K=0.1$, $M=1$, $Q=0.1$, $E=0.01$, $A=0.5$, $F=0.01$, $\gamma=\pi/3$, $\alpha=\pi/6$, $Gm=5$, $t=0.5$, $n=1$, $Up=0.5$, $Sr=1$.

Figures 2-10 exhibit the variation of the velocity distribution u versus normal coordinate y under the influence of Aligned magnetic field γ , Inclined parameter α , magnetic parameter M , Soret number Sr , Schmidt number Sc , chemical reaction parameter K , heat source/sink parameter Q , thermal Grashof number Gr and solutal Grashof number Gm . Figure 2 and 3 shows that effect of Aligned magnetic field parameter and Inclined parameter on velocity. It is observed that velocity is diminishes with increasing respective parameters. Figure 4 shows that, Velocity is increased with increasing values of Soret parameter (Sr). Figure 5 shows that the fluid flow is retarded due to imposition of the transverse magnetic field. The presence of magnetic field in an electrically conducting fluid introduces a force called Lorentz force which acts against the flow if the magnetic field is applied normal to the fluid flow. This type of resistive force tends to slow down the flow field. Thus our observation and physical reality are consistent. The porosity parameter on velocity distributions is depicted in Figure. 6. It is observed that the enhancing value of porosity parameter increases the velocity distributions. The improving values of porous medium increases the permeability; this can lead to improving the velocity profiles. Figure 7 clearly shows that there is a enhances in the fluid velocity when the Schmidt number Sc is increased which indicates the fact that the fluid velocity increases significantly due to high mass diffusivity. It is recalled that an increase in Sc means a decrease in molecular diffusivity. The influence of the heat source/sink parameter Q on velocity has been depicted in Figure 8. It is observed that an increase in the values of Q leads to a fall in the velocity.

Figure 9 and Figure 10 depict that thermal buoyancy force and solutal buoyancy force causes the flow to accelerate to a good extent near the plate. The Grashof number for heat transfer Gr signifies the relative effect of the thermal buoyancy force to the viscous hydrodynamic force in the boundary layer. As expected, it is observed that there is a rise in the velocity due to the enhancement of thermal buoyancy force. Also, as Gr increases, the peak values of the velocity increases rapidly near the porous plate and then decays smoothly to the free stream velocity. The Grashof number for mass transfer Gc defines the ratio of the species buoyancy force to the viscous hydrodynamic force. As expected, the fluid velocity increases and the peak value is more distinctive due to increase in the species buoyancy force. The velocity distribution attains a distinctive maximum value in the vicinity of the plate and then decreases properly to approach the free stream value. It is noticed that the velocity increases with increasing values of the Grashof number for mass transfer Gc . In the figure 11 expressed the effect of Casson fluid parameter λ . The resultant velocity is diminished with increasing values of Casson fluid parameter.

The variation of temperature field θ against y under the influence of heat sink Q , Prandtl number Pr and Radiation Parameter (R) are demonstrated in Figures 12-14. It is noticed from the figure 12 that there is a comprehensive fall in temperature for increasing heat sink within the fluid region. Figure 13 depicts the effect of Prandtl number on temperature profiles in presence of some selected fluids such as Hydrogen ($Pr = 0.68$), Air ($Pr = 0.71$), Carbon dioxide ($Pr = 0.76$) and Electrolytic solution ($Pr = 1$). From this figure, we observed that, an increase in the Prandtl number decreases the temperature of the flow field at all points. Due to the ratio of momentum diffusivity (kinematic viscosity) to thermal diffusivity. The similar behavior is observed in figure 14 in the case of Radiation parameter is increased.

Figures 15-17 demonstrate the variation of concentration field under the influence of the parameters Schmidt number (Sc), Soret Parameter (Sr), and Chemical reaction Parameter (K). Figure 15 shows that the concentration level of the fluid is decreased for increasing Schmidt number. This is consistent with the fact that an increase in Sc means a decrease of molecular diffusivity which results in a fall in the thickness of the concentration boundary layer. It is seen from Figure 16 that concentration level increases in presence of thermal diffusion. It is noticed from Figure 17 that there is a comprehensive fall in the concentration level of the fluid due to chemical reaction which indicates a reduction in the thickness of the boundary layer.

In all the tables (Skin friction, Nusselt Number and Sherwood number) Comparisons with previously published work Choudhury et al. [26] performed and the results are found to be in the excellent agreement.

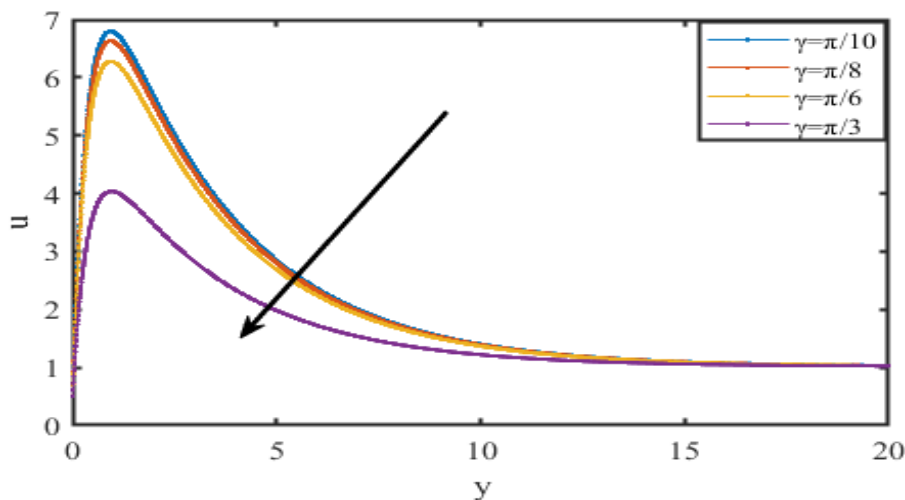


Figure 2: Effect of Aligned magnetic field (γ) on Velocity Profiles

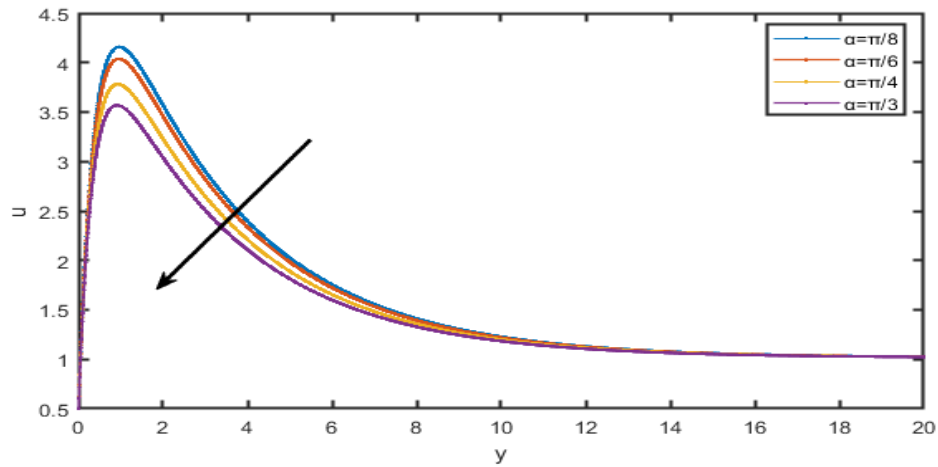


Figure 3: Effect of Inclined Parameter (γ) on Velocity Profiles

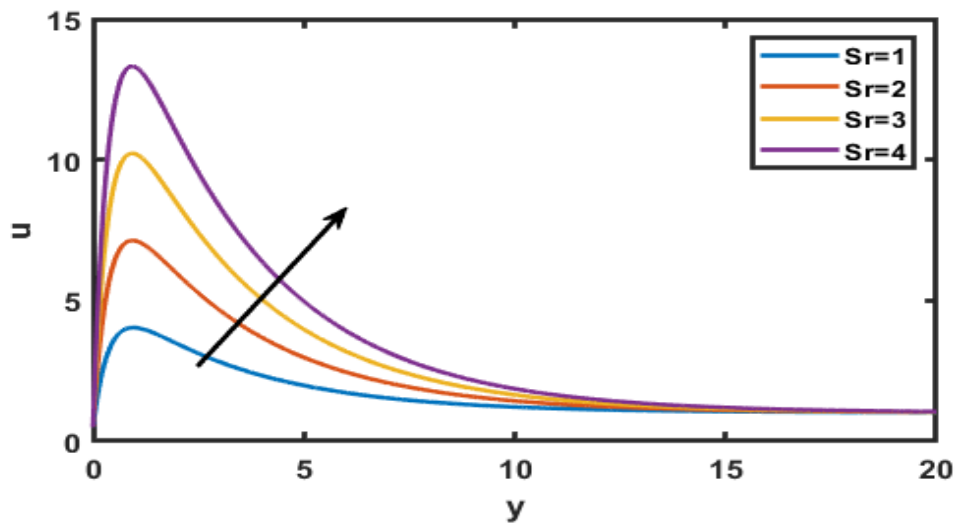


Figure 4: Effect of Soret parameter (Sr) on Velocity Profiles

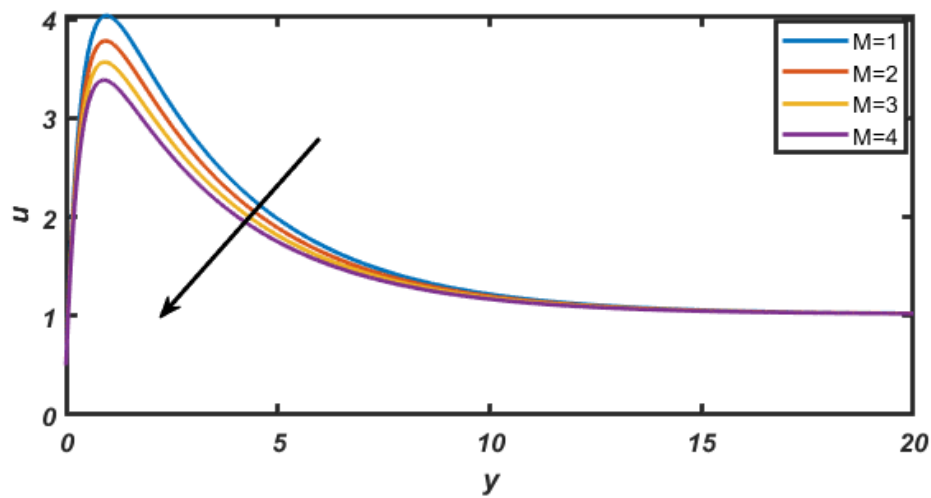


Figure 5: Effect of Magnetic field parameter (M) on Velocity Profiles

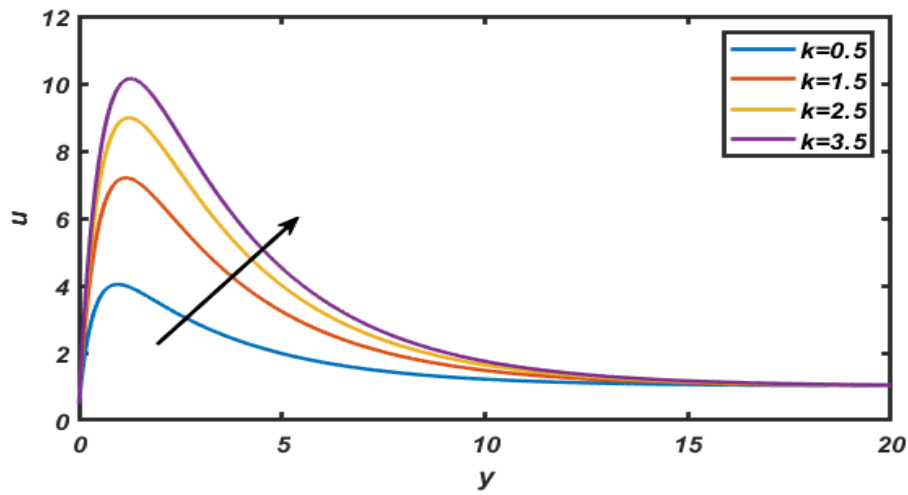


Figure 6: Effect of Porous media parameter (k) on Velocity Profiles

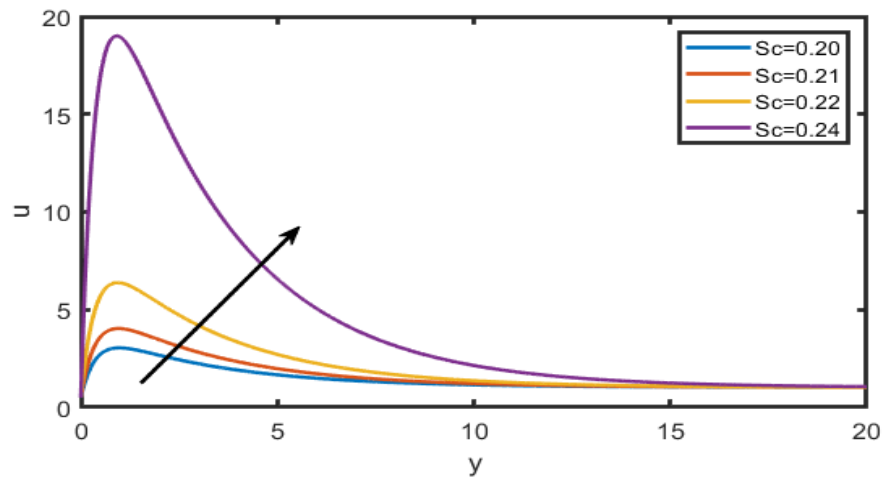


Figure 7: Effect of Schmidt number parameter (Sc) on Velocity Profiles

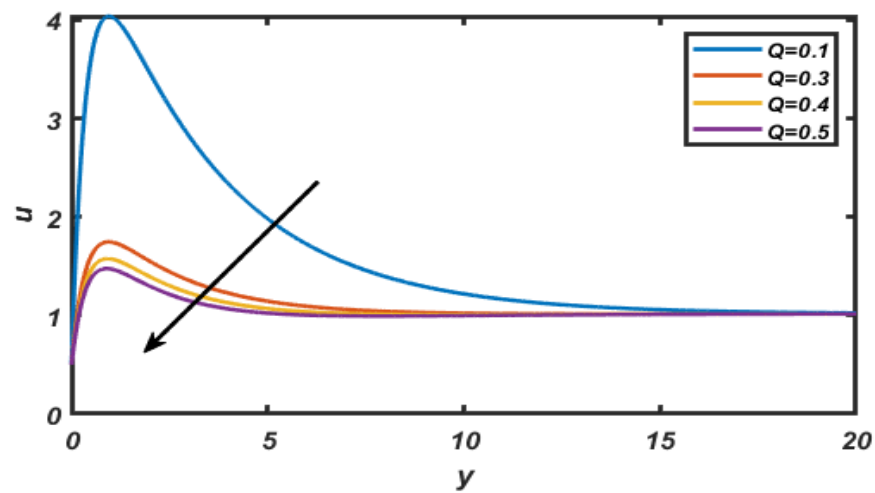


Figure 8: Effect of the heat source/sink parameter (Q) on Velocity Profiles

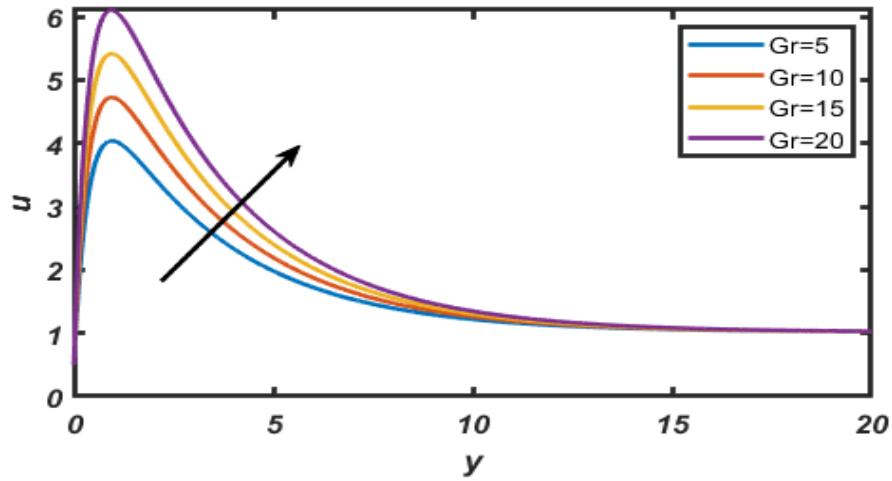


Figure 9: Effect of the Thermal Grashof number (Gr) on Velocity Profiles

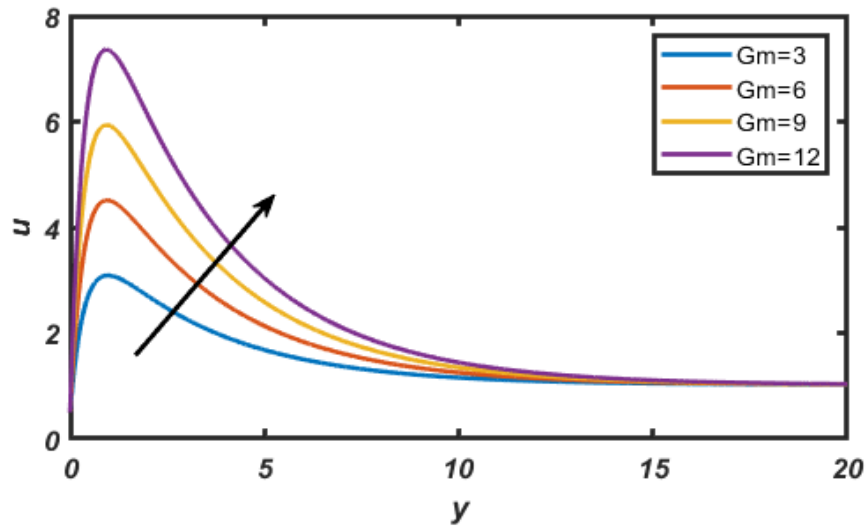


Figure 10: Effect of the Mass Grashof number (Gm) on Velocity Profiles

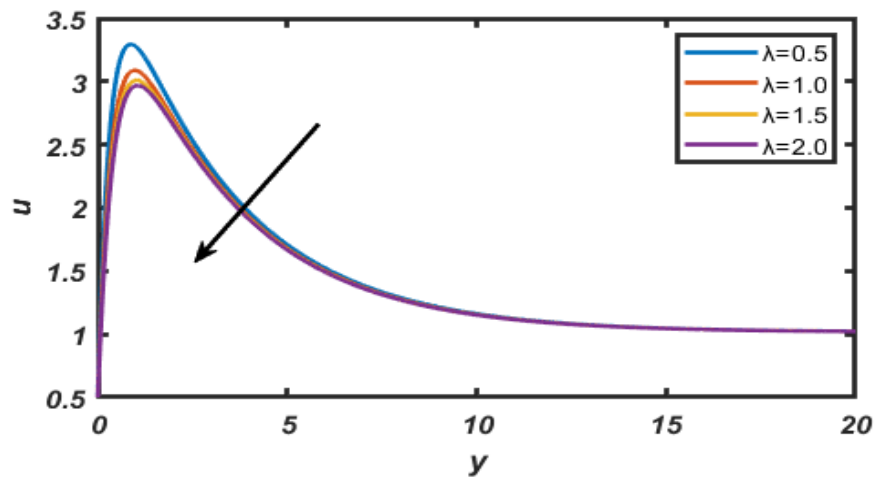


Figure 11: Effect of the Casson Fluid parameter (λ) on Velocity Profiles

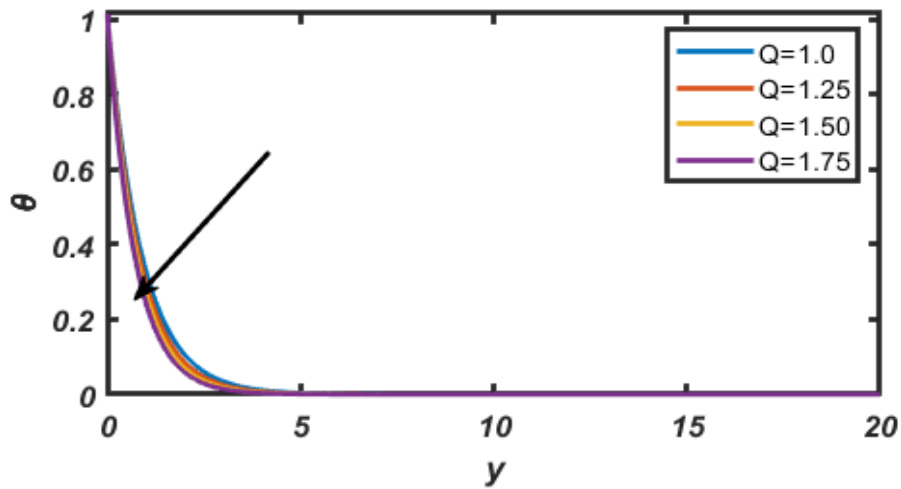


Figure 12: Effect of the Heat absorption (Q) on Temperature Profiles

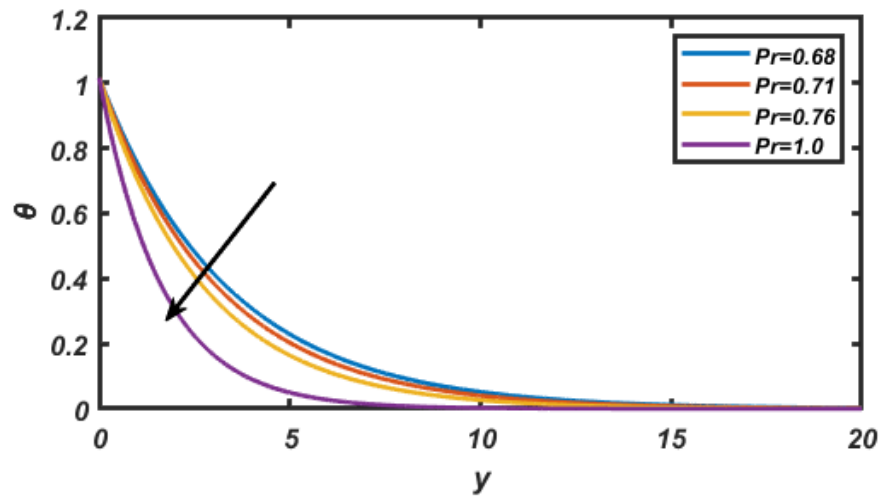


Figure 13: Effect of the Prandtl number (Pr) on Temperature Profiles

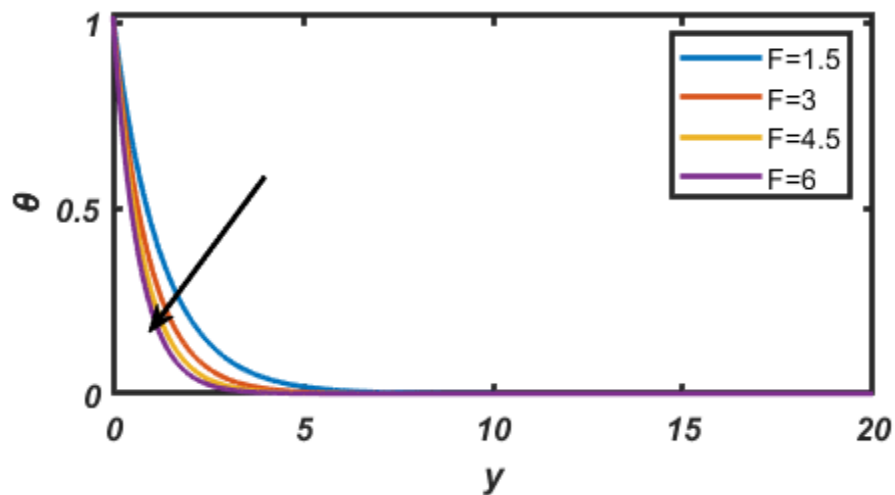


Figure 14: Effect of the Radiation Parameter (F) on Temperature Profiles

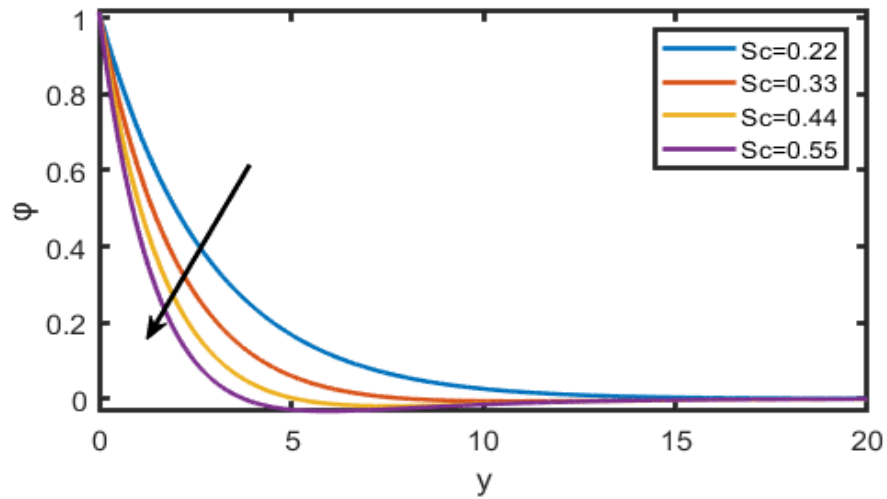


Figure 15: Effect of the Schmidt number (Sc) on Concentration Profiles

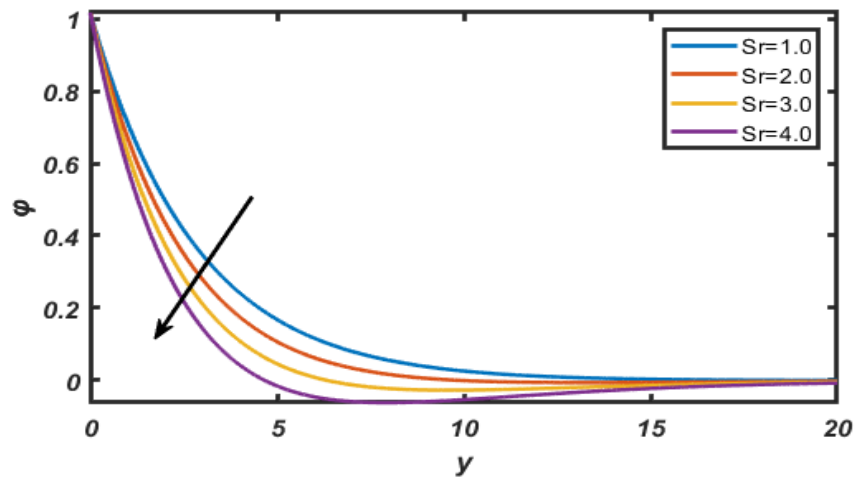


Figure 16: Effect of the Soret number (Sr) on Concentration Profiles

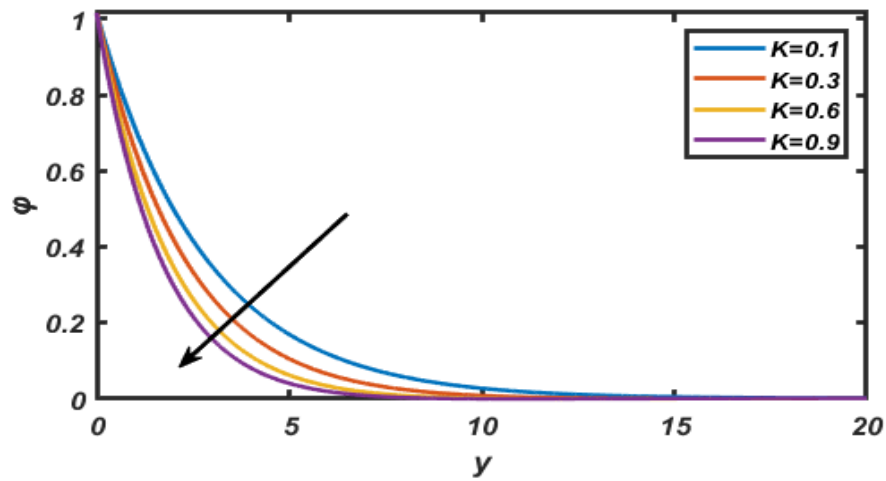


Figure 17: Effect of the Chemical reaction (K) on Concentration Profiles

Table 1.Skin friction

Sc	K	Q	Sr	τ
0.22	0.5	1	0.3	3.3717
0.3				3.2982
0.6				3.2148
0.6	0.1	1	0.3	3.3938
	0.2			3.3604
	0.3			3.3431
0.6	0.5	0	0.3	3.7057
		1		3.2148
		2		3.18807
0.6	0.5	1	1	3.2148
			1.5	3.5740
			2	3.6832

Table 2.Nusselt number

Q	Pr	t	Nu
1	0.71	0.5	-1.5796
2			-1.7797
3			-2.3370
1	0.71	0.5	-1.5796
	2		-3.4690
	7.0		-10.7271
1	0.71	0.1	-1.5823
		0.2	-1.5856
		0.3	-1.5880

Table 3.Sherwood Number

Q	K	Sr	Sh
1	1	1	-0.3995
2			-0.5409
3			-0.7564
1	0.1	1	-0.0864
	0.2		-0.1255
	0.3		-0.8443
1	1	1	-1.1686
		1.5	-1.0340
		2	-0.8995

Conclusion:

The present investigation leads to the following conclusions:

1. The fluid velocity decreases with the increase in Aligned magnetic field parameter, Inclined angle, Magnetic field parameter, Schmidt number, Casson fluid parameter and heat sink parameter whereas it is accelerated due to Porous media, Soret parameter, and thermal diffusion.
2. The fluid temperature drops with the increase in heat sink parameter, Prandtl number and Radiation parameter.
3. The concentration level of the fluid rises with the falls due to Schmidt number, soret parameter, and chemical reaction parameter.

References:

[1]. S. Shaw, R.S.R. Gorla, P. Murthy, Pulsatile Casson fluid flow through a stenosed bifurcated artery, Int. J. Fluid Mech. Res. 36 (2009) 43–63.

- [2]. S. Nadeem, RizwanUIHaq, Noreen Sher Akbar, Z.H. Khan, MHD three-dimensional Casson fluid flow past a porous linearly stretching sheet, *Alex. Eng. J.* 52 (2013) 577–682.
- [3]. T. Hayat, S.A. Shehzad, A. Alsaedi, Three-dimensional stretched flow of Jeffrey fluid with variable thermal conductivity and thermal radiation, *Appl. Math. Mech.* 34 (2013) 823–833.
- [4]. M. Thiagarajan, K. Senthilkumar, DTM-Pade approximants of MHD boundary-layer flow of a Casson fluid over a shrinking sheet, *USA Res. J.* 1 (2013) 1–7.
- [5]. S. Mukhopadhyay, Effects of slip on unsteady mixed convective flow and heat transfer past a stretching surface, *Chin. Phys. B.* 27 (2010) 256–307.
- [6]. K. Ahmad, R. Nazar, Magneto hydrodynamic three dimensional flow and heat transfer over a stretching surface in a viscoelastic fluid, *J. Sci. Technol.* 3 (2011) 145–155.
- [7]. K. Bhattacharyya, S. Mukhopadhyay, G.C. Layek, Slip effects boundary layer stagnation-point flow and heat transfer towards a shrinking sheet, *J. Heat Mass Transf.* 54 (2011) 308–313.
- [8]. Ahammad, N. & Chamkha, Ali & Krishna, M. Veera. (2021). Hall and ion slip impacts on unsteady MHD convective rotating flow of heat generating/absorbing second grade fluid. *Alexandria Engineering Journal*.60. 10.1016/j.aej.2020.10.013.
- [9]. Krishna, M. Veera & T, Prameela & BV, Swarnalathamma & Chamkha, Ali. (2018). Heat and mass transfer on MHD Chemically Reacting flow of a Micro-polar fluid through a Porous medium with Hall effects. *Special Topics & Reviews in Porous Media: An International Journal*. 9. 10.1615/SpecialTopicsRevPorousMedia.2018024579.
- [10]. Krishna, M. Veera. (2018). Heat and mass transfer on Unsteady MHD Oscillatory flow of Second grade fluid through porous medium between two vertical plates fluctuating Heat Source/Sink and Chemical react. *International Journal of Fluid Mechanics Research*.45. 10.1615/InterJFluidMechRes.2018024591.
- [11]. Krishna, M. Veera & Anand, PVS & Chamkha, Ali. (2018). Heat and Mass transfer on Free Convective flow of a Micro-polar fluid through a Porous surface with Inclined Magnetic Field and Hall effects. *Special Topics & Reviews in Porous Media: An International Journal*. 10. 10.1615/SpecialTopicsRevPorousMedia.2018026943.
- [12]. Krishna, M. Veera & Jyothi, Kamboji & Chamkha, Ali. (2020). Heat and mass transfer on MHD flow of Second grade fluid through porous medium over a semi-infinite vertical stretching sheet. *Journal of Porous Media*.23. 10.1615/JPorMedia.2020023817.
- [13]. Obulesu M, Raghunath K, and Sivaprasad R: Radiation absorption effects on MHD Jeffrey fluid flow past a vertical plate through a porous medium in conducting field, *ANNALS of Faculty Engineering Hunedoara-International Journal of Engineering*, Tome XIX(2021), Fascicule 1(February), PP:69-75.
- [14]. K. Raghunath, M. Obulesu and R. Sivaprasad "Heat and mass transfer on an unsteady MHD flow through porous medium between two porous vertical plates", *AIP Conference Proceedings* 2220, 130003 (2020) <https://doi.org/10.1063/5.0001103>.
- [15]. M. Obulesu, K. Raghunath, and R. Sivaprasad, Hall current effects on MHD convective flow past a porous plate with thermal radiation, chemical reaction with radiation absorption, *AIP Conference Proceedings* 2246, 020003 (2020) <https://doi.org/10.1063/5.0014423>.

- [16]. K.Raghunath, R.Siva Prasad, and G.S.S.Raju, Heat and mass transfer on MHD flow of Non-Newtonian fluid over an infinite vertical porous plate, International Journal of Applied Engineering Research ISSN 0973-4562 Volume 13, Number 13 (2018) pp. 11156-11163.
- [17]. K.Raghunath, R.Siva Prasad, and G.S.S.Raju, Heat and mass transfer on Unsteady MHD flow of a second grade fluid through porous medium between two vertical plates, JUSPS-B Vol. 30(2), 1-11 (2018).
- [18]. K.Raghunath, R.Siva Prasad, and G.S.S.Raju, Hall Effects on MHD Convective Rotating Flow of Through a Porous Medium past Infinite Vertical Plate, Annals of Pure and Applied Mathematics, Vol. 16, No. 2, 2018, 353-263.
- [19]. K.Raghunath, M. Veerakrishna, R.Siva Prasad, and G.S.S.Raju, Heat and Mass Transfer on Unsteady MHD Flow of a Visco-Elastic Fluid Past an Infinite Vertical Oscillating Porous Plate, British Journal of Mathematics & Computer Science, 17(6): 1-18, 2016.
- [20]. G V Nagendra Prasad, G Nagesh, K Raghunath, Dr R Siva Prasad, MHD flow of a Visco-elastic fluid over an unbounded rotating porous plate with Heat source and Chemical reaction, International Journal of Applied Engineering Research ISSN 0973-4562 Volume 13, Number 24 (2019) pp. 16927-16938.
- [21]. G Suresh babu, G Nagesh, K Raghunath, Dr R Siva Prasad, Finite Element Analysis of Free Convection Heat Transfer Flow in a Vertical Conical Annular Porous Medium, International Journal of Applied Engineering Research ISSN 0973-4562 Volume 14, Number 1 (2019) pp. 262-277.
- [22]. Prabhakar Reddy B, JeftaSunzu P (2016) Thermal radiation and viscous dissipation effects on MHD heat and mass diffusion flow past a surface embedded in a porous medium with chemical reaction. Int J Math Appl 4(2):91–103
- [23]. Okelo JA, Imbusi MN, Awour KO, Kalaal A, Onchaga CA (2015) Viscous incompressible heat generating fluid flow past an infinite porous plate with radiation absorption. Int J SciEng Res 3(10):51–65
- [24]. Vedavathi N, Ramakrishna K, Jayarami RK (2015) Radiation and mass transfer effects on unsteady MHD convective flow past an infinite vertical plate with Dufour and solet effects. Ain Shams Eng J 6:363–371
- [25]. Gnaneswara RM (2014) Thermal radiation and chemical reaction effects on MHD mixed convective boundary layer slip flow in a porous medium with heat source and Ohmic heating. EurPhys J Plus 129(41):1–17.
- [26]. K. Choudhury and N. Ahmed (2018), Solet Effect on Transient MHD Convective Flow past a Semi-infinite Vertical Porous Plate with Heat Sink and Chemical Reaction, Applications and applied mathematics, Vol 13, pp.839-85.
- [27]. Rajakumar KVB, Balamurugan KS, Ramana Murthy CV (2018) Radiation absorption and viscous-dissipation effects on magneto hydrodynamic free convective flow past a semi-infinite, moving, vertical, porous plate. Int J Fluid Mech Res 45(5):439–458.
- [28]. Rajakumar KVB, Balamurugan KS, Ramana Murthy CV (2018) The Radiation, dissipation and Dufour effects on MHD free convection Casson fluid flow through a vertical Oscillatory porous plate with Ion-slip current. Int J Heat Technol 36(2):494–508
- [29]. Cramer, K.P., Pai, S.I.: Magneto Fluid Dynamics for Engineers and Applied Physics. McGraw-Hill Book Co, New York (1973)
- [30]. Grief, G., Habib, I.S., Lin, L.C.: Laminar convection of a radiating gas in a vertical channel. J. Fluid Mech. 45, 513–520 (1971)

[31]. Obulesu M and Sivaprasad R: MHD double diffusive visco-elastic fluid flow past an infinite vertical porous plate under the influence of radiation absorption, AIP Conf. Proc. 2246, 020069-1–020069-8; <https://doi.org/10.1063/5.0014428>.

[32]. Obulesu M and Sivaprasad R: Hall current effects on MHD convective flow past a porous plate with thermal radiation, chemical reaction with thermophoresis, ANNALS of Faculty Engineering Hunedoara-International Journal of Engineering, Tome XVII(2020),Fascicule 3(August),PP:205-212.

[33]. Obulesu M and Sivaprasad R: Joule heating and thermal diffusion effect on MHD fluid flow past a vertical porous plate embedded in a porous medium, Print version ISSN 0970 6577, online version ISSN 2320 3226 DOI: 10.5958/2320-3226.2019.00011.0, PP:117-134, Bulletin of Pure and Applied Sciences, Vol. 38E (Math & Stat.), No.1,January-June 2019.

APPENDIX

$$N = \frac{1}{k} + M \sin^2 \gamma \quad \lambda_1 = \left(1 + \frac{1}{\lambda}\right) m_1 = \frac{\text{Pr} + \sqrt{\text{Pr}^2 + 4\chi \text{Pr}}}{2} \quad m_2 = \frac{\text{Pr} + \sqrt{\text{Pr}^2 + 4(\chi + n)\text{Pr}}}{2}$$

$$m_3 = \frac{\text{Sc} + \sqrt{\text{Sc}^2 + 4\text{Sc}K}}{2} \quad m_4 = \frac{\text{Sc} + \sqrt{\text{Sc}^2 + 4(K + n)\text{Sc}}}{2} \quad m_5 = \frac{1 + \sqrt{1 + 4N}}{2}$$

$$m_6 = \frac{1 + \sqrt{1 + 4(N + n)}}{2} \quad A_1 = \frac{A m_1 \text{Pr}}{m_1^2 - \text{Pr} m_1 - (n + \chi)\text{Pr}} \quad A_2 = 1 - A_1$$

$$A_3 = \frac{\text{Sc} S r m_1^2}{m_1^2 - \text{Sc} m_1 - \text{Sc} K} \quad A_4 = 1 - A_3 \quad A_5 = \frac{A A_3 \text{Sc} m_1 - A_1 \text{Sc} S r m_1^2}{m_1^2 - \text{Sc} m_1 - \text{Sc}(K + n)} \quad A_6 = \frac{-A_2 \text{Sc} S r m_2^2}{m_2^2 - \text{Sc} m_2 - \text{Sc}(K + n)}$$

$$A_7 = \frac{A A_4 \text{Sc} m_3}{m_3^2 - \text{Sc} m_3 - \text{Sc}(K + n)} \quad A_8 = 1 - (A_5 + A_6 + A_7)$$

$$A_9 = \frac{-Gr \cos \alpha - A_3 G m \cos \alpha}{m_1^2 \lambda_1 - m_1 - N} \quad A_{10} = \frac{-A_4 G m \cos \alpha}{m_3^2 \lambda_1 - m_3 - N} \quad A_{11} = U_p - (1 + A_9 + A_{10})$$

$$A_{12} = \frac{-A_1 Gr \cos \alpha - A_5 G m \cos \alpha + A A_9 m_1}{m_1^2 \lambda_1 - m_1 - (N + n)} \quad A_{13} = \frac{-A_2 Gr \cos \alpha - A_6 G m \cos \alpha}{m_2^2 \lambda_1 - m_2 - (N + n)}$$

$$A_{14} = \frac{-A_7 G m \cos \alpha + A A_{10} G m m_3}{m_3^2 \lambda_1 - m_3 - (N + n)} \quad A_{15} = \frac{-A_8 G m \cos \alpha}{m_4^2 \lambda_1 - m_4 - (N + n)} \quad A_{16} = \frac{A A_{11} m_5}{m_5^2 \lambda_1 - m_5 - (N + n)}$$

$$A_{17} = 1 - (A_{12} + A_{13} + A_{14} + A_{15} + A_{16})$$